PAPER

NJC
www.rsc.org/njc

Topological ferrimagnetic behavior of one new chain with the new AF/F/F′/F′/F alternating sequence

Joan Cano,*[a] Yves Journaux,[a] Mohamed A. S. Goher,[b] Morsy A. M. Abu-Youssef,[b] Franz A. Mautner,[c] Guido J. Reiß,[d] Albert Escuer*[e] and Ramon Vicente[e]

[a] *Laboratoire de Chimie Inorganique (CNRS UMR 8613), Université de Paris-Sud, F-91405 Orsay, France. E-mail: joan.cano@qi.ub.es*
[b] *Chemistry Department, Faculty of Science, Alexandria University, PO Box 426 Ibrahimia 21321 Alexandria, Egypt*
[c] *Institut für Physikalische und Theoretische Chemie, Technische Universität Graz, A-8010 Graz, Austria*
[d] *Institut für Anorganische Chemie und Strukturchemie, Heinrich-Heine-Universität Düsseldorf, Universitätstrasse-1, D-40225 Düsseldorf, Germany*
[e] *Departament de Química Inorgànica, Universitat de Barcelona, Diagonal 647, 08028 Barcelona, Spain. E-mail: albert.escuer@qi.ub.es*

Received (in Montpellier, France) 25th March 2004, Accepted 25th June 2004
First published as an Advance Article on the web 14th December 2004

An azido-bridged chain with formula $[Mn(Menic)(N_3)_2]_n$, where Menic is methylnicotinate, was prepared and studied from the magnetic point-of-view. This compound crystallizes in the monoclinic system, space group $P21/a$, with $a = 15.556(2)$, $b = 16.831(2)$, $c = 17.595(2)$ Å, $\beta = 110.80(1)^\circ$ and $Z = 10$. The structure consist of a one-dimensional system in which each manganese atom is bridged by two azido ligands in a *trans* arrangement. Along the chain there are four double end-on azido bridges followed by one double end-to-end azido bridge. This unusual kind of alternation leads to a new one-dimensional magnetic behavior, which has been studied by means of susceptibility and single crystal ESR measurements. The magnetic response has been reproduced by Monte Carlo simulations and exact laws following the classical approach. The characteristic signature of the magnetic behavior has allowed us to determine the three different magnetic coupling constants present in this system. These results have been analyzed in the framework of a theoretical and experimental magneto-structural correlation.

DOI: 10.1039/b404622f

Introduction

Research on the magnetic properties of azido-bridged systems is a growing field that in recent years has provided a large number of uncommon magnetic systems.[1] The ability of the azido bridge to coordinate in the end-to-end mode (EE, generally associated with antiferromagnetic coupling) or end-on mode (EO, generally associated to ferromagnetic coupling) is the key of the versatility of this ligand. In addition, the azido bridge allows molecular compounds with a wide range of nuclearities[1,2] but easily tends to give extended systems having 1D to 3D dimensionalities.[1,3] Besides the large number of magnetic topologies obtained, the compounds in which the two kinds of coordination modes are simultaneously present deserve particular attention, as they give alternating systems with unusual or in some cases, unprecedented, magnetic behavior. As an example, a few 3D networks[1,4] containing both EE and EO azido ligands have been characterized, together with several 2D systems[1] that often exhibit long-range order at moderately low temperatures. Focusing our attention on the 1D derivatives, the compounds having the general formula $[Mn(R\text{-}py)_2(N_3)_2]_n$ in which R-py is a pyridinic ligand with an R group attached generally in the *meta* or *para* positions, form the most complete series reported to date, with gradual changes in the topology of the system (see Scheme 1). This series of compounds goes from compounds containing only EO bridges[5] to compounds containing only EE bridges[3d,5a,6] with F or AF magnetic response, respectively (topologies I and VI in Scheme 1), though systems in which the ratio of EE : EO bridges is 2 : 1 (V),[7] 1 : 1 (III, IV)[1,3e,5a,8] or 1 : 4 (II)[7a] are also known. This gradual increase of the AF/F interactions along the chain provides interesting material to study unusual magnetic properties such as the ferrimagnetic response of type V compounds,[7] the EPR of chains with a gradual change of the superexchange and dipolar interactions[5a] or to develop theoretical studies to explain the new properties.[5a,6,7b]

In this work we present the full magnetic characterization by means of susceptibility and single-crystal ESR measurements of the $[Mn(Menic)_2(N_3)_2]_n$ one-dimensional system (**1**), in which Menic is the methylnicotinate ligand. This compound represents the only known example of a type II system.[7a] In this paper, we try to analyze the magnetic behavior of this family of compounds. However, we know that the explanation of the macroscopic properties of matter resulting from the interplay of a large number of atoms is very complex. Most problems in statistical physics are too complicated to permit exact solutions and, frequently, the accuracy of the results is very uncertain due to the use of uncontrolled approximations. Monte Carlo simulation is an important technique used to tackle this problem.

In recent years, the study of one-dimensional spin-Heisenberg Hamiltonians has received considerable attention by chemists and physicists. One reason for this is that these systems provide excellent examples for the development of suitable theoretical models that afford a better understanding of the magnetic behavior in extended lattices. In this way, new

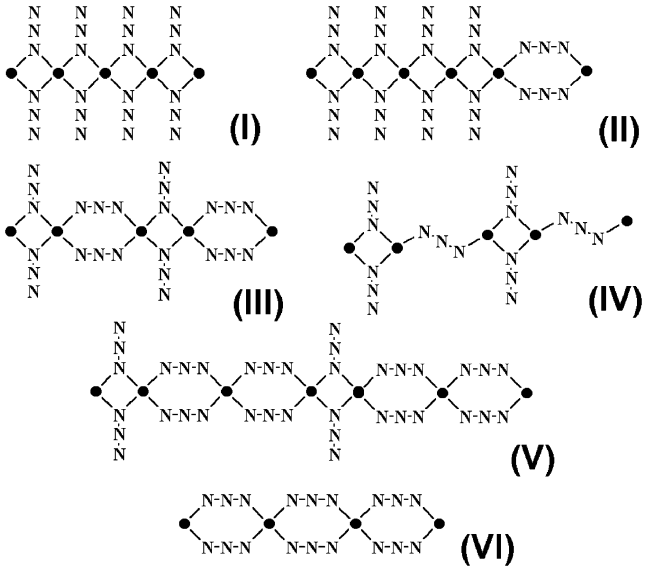

Scheme 1

classes of low dimensional magnetic materials have been obtained, which require the development of new theoretical models in order to describe correctly their magnetic properties.[9] In this case, studies of antiferromagnetic chains have been particularly fruitful.

Antiferromagnetic interactions are far more usual in nature than ferromagnetic ones. Some bimetallic chains, in which a non-compensation of the local spins occurs, are able to present a magnetic behavior quite similar to that of ferromagnetic chains.[10] These are the reasons for the great interest developed during the last decades in these compounds. From a theoretical point of view, these systems are not easy to study. The first studies on this subject date from the 1980s.[11,12] Other studies using more powerful methods, such as quantum Monte Carlo (QMC) and density matrix group renormalization (DMRG), were not published until the late 1990s.[13,14] Only regular one-dimensional systems had been studied so far, but recently, Ovchinnikov *et al.* have studied more complex one-dimensional interaction topologies.[15] Although all these studies have been performed on hetero-bimetallic chains, this phenomenon can also be present in homo-metallic chains with special interaction topologies.[7b]

Fischer,[16] considering that quantum effects are negligible in $S = 5/2$ systems, estimated analytically the dependence of the magnetic susceptibility with temperature. In a similar way, Abu-Youssef *et al.*[7b] and Cortés *et al.*[17] have studied several $S = 5/2$ alternating chains. The application of the same technique on the higher dimensionality systems was shown to be very complicated, which is reflected in the fact that there are only exact laws for square and honeycomb planes.[18] Even these laws do not reproduce very well the magnetic properties of the systems having these topologies.[19]

Recently, other types of techniques have been applied to analyze the magnetic properties of extended systems, such as the QMC simulations[15,20–28] and the DMRG approach,[29–34] allowing quantum results on large systems to be obtained, which is not possible by an exact diagonalization of the energy matrix obtained from the microstate basis.

In this work, we have deduced analytical expressions for the AF/F/F/F/F and AF/F/F′/F′/F alternating one-dimensional models using the classical spin approach. These laws have allowed us to analyze the magnetic susceptibility *vs.* temperature curves for compound **1**. The results have been checked by a Monte Carlo simulation based on the Metropolis algorithm[27,35] and compared with the predictions from DFT calculations.[36]

Experimental

Infrared spectra (4000–200 cm^{-1}) were recorded from KBr pellets on a Nicolet 520 FTIR spectrophotometer. Magnetic measurements were performed with a Quantum Desing instrument with a SQUID detector, working in the temperature range of 300–2 K under an external magnetic field of 0.01 T. Diamagnetic corrections were estimated from Pascal's Tables. ESR spectra were recorded at the X-band frequency with a Bruker ES200 spectrometer equipped with an Oxford liquid-helium cryostat for variable temperature work and automatic goniometer for single-crystal measurements.

Synthesis

$[Mn(Menic)_2(N_3)_2]_n$ (**1**) was synthesized by mixing a methanolic solution (30 mL) of manganese(II) chloride tetrahydrate (0.99 g, 5 mmol) and 1.21 g (10 mmol) of methylnicotinate dissolved in 20 mL methanol, followed by dropwise addition of a saturated aqueous solution of sodium azide (0.65 g, 10 mmol). The final solution was filtered off and then was left to stand in the dark for 2 weeks, which led to the growth of needle-shaped colorless crystals of **1**. Yield *ca.* 60%. Anal. calcd for $C_{14}H_{14}MnN_8O_4$: C, 40.7; H, 3.4; N, 27.1; Mn, 13.3; found: C, 40.6; H, 3.5; N, 27.1; Mn, 13.3

The IR spectrum of the solid complex shows bands attributable to the methylnicotinate ligand at normal frequencies. In the 2000–2150 cm^{-1} region the complex shows two very strong and split bands assigned to the asymmetric stretching vibrations (ν_{as} N_3) centered at 2100 (vs) and 2073 (vs) cm^{-1}. No band could be attributed to the (ν_s N_3) mode in the 1280–1360 cm^{-1} region, while the two bands at 2100 and 2073 cm^{-1} indicate the presence of two different symmetric and asymmetric azido groups. In the far-infrared region a few bands were observed at 216, 244, 342, 362 and 431 cm^{-1} and could be tentatively assigned to the $M–N_{ligand}$ and $M–N_{N_3}$ vibrations.

X-Ray crystallography

A colorless crystal (0.30 × 0.60 × 1.00 mm^3) was mounted on a STOE-IPDS diffractometer equipped with graphite-monochromated MoKα radiation (λ = 0.71073 Å). Intensity data were corrected for Lorentz and polarization effects. Data reduction and a numerical absorption (X-SHAPE: min/max transmission: 0.604/0.803) correction were performed with the STOE-IPDS software[37] and structure solution and refinements

Table 1 Crystal data and structure refinement details for **1**

Chemical formula	$C_{14}H_{14}MnN_8O_4$
Formula weight	413.27
Space group	$P21/a$ (No. 14)
a/Å	15.556(2)
b/Å	16.831(2)
c/Å	17.595(2)
β/deg	110.80(1)
U/Å^3	4306.7(9)
Z	10
D_{calcd}/g cm^{-3}	1.592
T/°C	20
v/Å	0.71073
μ/mm^{-1}	0.807
$R(F)^a$	0.0641
$wR(F^2)^a$	0.1917

^{a} $R(F_o) = \Sigma F_o - F_c/\Sigma F_o$; $\omega R(F_o)^2 = \{\Sigma[\omega((F_o)^2 - (F_c)^2)^2]/\Sigma[\omega(F_o)^4]\}^{1/2}$.

Table 2 Selected bond lengths (Å) and angles (°) for **1**

Manganese environment			
Mn1–N1	2.302(3)	Mn2–N11a	2.232(3)
Mn1–N11	2.236(3)	Mn3–N4	2.298(4)
Mn1–N21	2.243(3)	Mn3–N5	2.321(3)
Mn2–N2	2.308(3)	Mn3–N31	2.219(3)
Mn2–N3	2.316(3)	Mn3–N41	2.215(5)
Mn2–N21	2.224(3)	Mn3–N51	2.201(5)
Mn2–N31	2.231(3)	Mn3–N53	2.224(5)
Mn2–N41	2.239(3)		
Mn_2N_2 rings			
N11–Mn1–N21a	78.6(1)	Mn1–N11–Mn2	101.1(1)
N11a–Mn1–N21	78.6(1)	Mn1–N21–Mn2	101.1(1)
N21–Mn2–N11a	79.1(1)	Mn2–N31–Mn3	100.7(1)
N31–Mn2–N41	79.0(1)	Mn2–N41–Mn3	100.5(2)
N31–Mn3–N41	79.8(1)		

conducted with SHELXTL/PC[38] and SHELXL-97,[39] respectively. Of the 17574 reflections collected, 6593 were observed with $I > 2\sigma(I)$, $R_{int} = 0.0671$; twin ratio = 0.244/0.756(1); twin matrix: {0.19 0 −0.81, 0 −1 0, −1.19 0 −0.19}; 612 refined parameters; $\rho_{min/max} = -1.94/1.80$ e Å^{-3}. All non-hydrogen atoms were refined anisotropically and hydrogen atoms were included by a riding model. Further crystallographic data are given in Table 1.† Selected bond parameters are summarized in Table 2.

Monte Carlo calculation methodology

In the canonical ensemble the average magnetization $\langle M \rangle$ is defined as:

$$\langle M \rangle = \frac{\sum_{i=1}^{\infty} M_i e^{-E_i/T}}{\sum_{i=1}^{\infty} e^{-E_i/T}} \quad (1)$$

As mentioned before, it is generally not possible to compute exactly this parameter due to the infinite number of configurations. The basic idea of the Monte Carlo technique is to approximate eqn. (1), where the sum runs over all states, by a partial sum over a subset of characteristic configurations N.

In the limit of $N \rightarrow \infty$, the resulting equation is identical to eqn. (1). One possibility is to choose randomly the configurations for the subset. This is the simple sampling variant of the Monte Carlo simulation. But due to the rapidly varying exponential function in the Boltzmann distribution, most of the chosen configurations make a negligible contribution to the sum since E_i is relatively large and consequently biases the calculation of the average quantities. Therefore, the Monte Carlo simulations were performed using the Metropolis algorithm,[35] which generates a sampling of states following the Boltzmann distribution that preferentially contains configurations that make an important contribution at the given temperature T. The magnetic susceptibility, χ_M, is related to the fluctuations of the magnetization[40] (see eqn. (2))

$$\chi_M T = N\beta^2/KT(\langle M^2 \rangle - \langle M \rangle^2) \quad (2)$$

where $\langle M \rangle$ and $\langle M^2 \rangle$ are the mean values of M and M^2, respectively, M being the magnetization.

All the simulations are done on a finite sample, which introduces systematic errors. First, to minimize the edge perturbation and to speed up the convergence toward the infinite lattice limit, periodic boundary conditions have been used.[27] In order to obtain reliable results, the optimal size of the samples has been determined by performing simulations at different system sizes. Finally, a 200 site sample has been used. This sample is eight times larger than the minimum size that did not present any finitesize effects for the reduced temperature range $T/|J|$ studied.

We performed 5×10^5 Monte Carlo steps per site and the first 5×10^4 were discarded as the initial transient stage.[27] To avoid freezing of the spin configuration[27] we have used a low cooling rate according to the following equation:

$$T_{i+1} = 0.98 \times T_i \quad (3)$$

where T is the temperature.

Results and discussion

Description of the structure

The structure, which has been published previously,[7a] consists of one dimensional arrangement of Mn^{II} ions linked by double azido bridges. The coordination sphere of the manganese atoms contains two *trans*-pyridinic ligands and four N atoms from four different azido ligands. The azido ligands show end-on coordination mode between Mn(1) and Mn(2) and also between Mn(2) and Mn(3), whereas between Mn(3) and Mn(3′) they show the end-to-end mode (Fig. 1).

Bond parameters for the EO azido bridges are quite similar and agree with the typical values reported to date in related systems: Mn(1)–N(11)–Mn(2) and Mn(1)–N(21)–Mn(2) are 101.1(1)° and Mn(2)–N(31)–Mn(3) and Mn(2)–N(41)–Mn(3) are 100.5(1)° and 100.7(2)°, respectively. Bond angles in the Mn(3)···Mn(3′) region are 130.6(4)° for Mn(3)–N(51)–N(52) and 127.6(4)° for Mn(3)–N(53)–N(52′). The fragment $Mn(NNN)_2Mn$ shows a small chair distortion evaluated as 8.2° between the plane defined by the two azido ligands and the N(53)–Mn(3)–N(51) plane. The singular arrangement of the azido coordination modes gives a system with four EO bridging units followed by one EE, which repeats along the chain. The reason for this uncommon alternation may be envisaged from the values of the N–Mn–N bond angles determined by the pyridinic ligands: the N(1)–Mn(1)–N(1′) bond angle is 180°, but due to steric hindrance N(2)–Mn(2)–N(3) has a value of 176.0(1)° and the next N(4)–Mn(3)–N(5) bond angle distorts, having a value of only 168.0(1)°. This distortion cannot continue indefinitely and the chain relaxes the steric hindrance by means of an EE fragment.

The Mn···Mn distances in the EO units are 3.426(1) and 3.450(1) Å whereas they reach 5.166(2) Å in the EE unit. The chains are well isolated by the large pyridinic ligands, the minimum Mn···Mn interchain distance being 10.767(1) Å.

† CCDC reference numbers 136998. See http://www.rsc.org/suppdata/nj/b4/b404622f/ for crystallographic data in .cif or other electronic format.

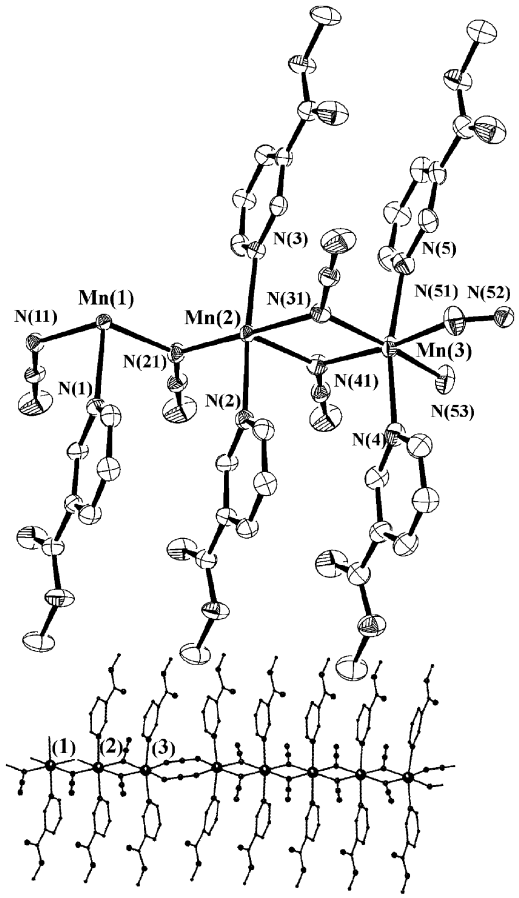

Fig. 1 Top: atom numbering scheme of the asymmetric unit of compound **1**. Bottom: view of the complete sequence of EE-EO azido bridges along the chain.

Susceptibility measurements and powder ESR spectra

The plot of the magnetic data over 300–2 K is shown in Fig. 2. The general behavior is quite uncommon, with a room temperature $\chi_M T$ value of 4.27 $cm^3\,K\,mol^{-1}$, which decreases continuously down to a minimum of 3.77 $cm^3\,K\,mol^{-1}$ at 60 K, reaches a sharp maximum at 10 K (4.47 $cm^3\,K\,mol^{-1}$) and below this temperature tends to zero. Magnetization measurements performed at 2 K indicate that the compound tends to a surprising saturation value equivalent to three electrons for each manganese atom.[7a] The magnetic behavior at low temperatures can be due to dipolar interactions between large spins (intra and interchain) or to the special interaction

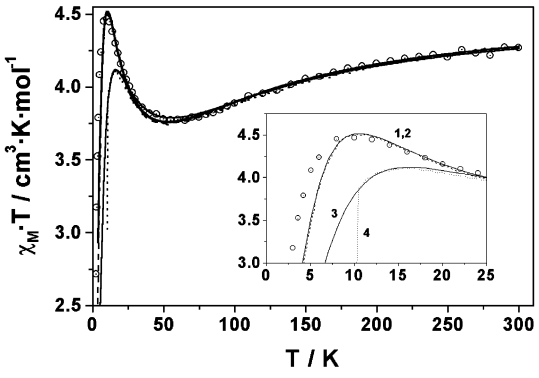

Fig. 2 $\chi_M T$ *vs.* T plot for **1**. The circles corresponds to the experimental data, the bold lines and dashed lines to the theoretical (eqns. (10) and (13)) and Monte Carlo simulations for the parameters that provide the best agreement with the magnetic data for the Hamiltonians expressed in eqns. (4) (plots 3, 4) and (11) (plots 1, 2).

topology shown by **1**. In the Monte Carlo simulations we have analyzed these possibilities.

The room temperature polycrystalline powder X-band EPR spectrum shows a broad band with a peak-to-peak width ΔH_{pp} = 422 G centered at g = 2.031. The linewidth of the spectra of one-dimensional compounds is the result of two opposing contributions: intrachain superexchange interactions, which tend to narrow the lines, and dipolar interactions, which tend to broaden them.[41] In similar one-dimensional systems, the value of the coupling constant is much greater for the end-to-end bridges than for the end-on ones and the dipolar interactions are mainly determined by the Mn···Mn distance: the shorter the distance the stronger the interaction. In qualitative terms exchange narrowing becomes dominant for the title compound, which shows very short Mn···Mn distances of 3.426 and 3.450 Å and only one end-to-end bridge for every four end-on bridges.

The comparison of the linewidth for the different topological possibilities pointed out in Scheme 1, in the comparable series of $[Mn(R\text{-}py)(N_3)_2]$ 1D derivatives, is interesting: for the compound with only double end-on bridges, topology I, the room temperature linewidth is 750 G and g = 2.05; for topology II with one double EE bridge for every four EO bridges the linewidth is 422 G and g = 2.03; for topologies III and IV with alternating double EE and EO bridges the linewidth is 220 G and g = 2.02; for topology V with two double EE for each EO bridge the linewidth lies between 124–154 G and g = 2.00; lastly, for compounds with only double EE bridges (topology VI) the linewidth reduces to a value close to 50 G and g = 2.00. These results correlate with a gradual increase of the superexchange interaction with a simultaneous decrease in dipolar interactions for the different kinds of chains. On cooling, the linewidth of the signal increases slightly down to 150 K; below this temperature both linewidth and g factor increases gradually to reach 743 G and 2.076, respectively (Fig. 3).

Single-crystal ESR experiments

ESR properties of quasi-ideal Heisenberg 1-D manganese antiferromagnets have been studied for several systems, mainly for $[(CH_3)_4N)][MnCl_3]$ (TMMC).[19] Recently, we have reported a single-crystal study for several chains with formula $[Mn(R\text{-}py)_2(N_3)_2]_n$ having topologies I, III and VI (F homogeneous, alternating F/AF and homogeneous AF systems, respectively). On the basis of the structural data and of the variation of the linewidth observed in the powder EPR spectra for the title compound, single-crystal measurements were performed, in order to characterize in more detail the spin dynamics of this new system and to complete the ESR study in a large series of related chains.

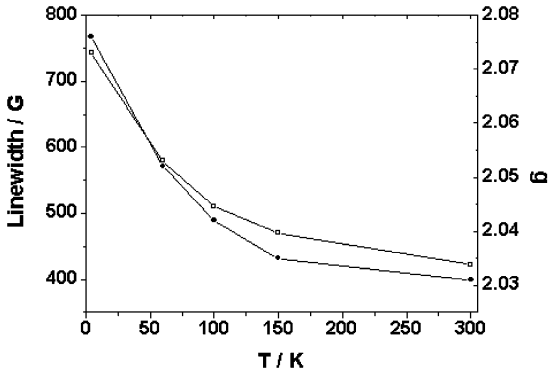

Fig. 3 Thermal dependence of the g value (solid circles) and the peak-to-peak linewidth ΔH_{pp} (open squares) for $[Mn(Menic)_2(N_3)_2]_n$ (**1**) at room temperature and at the X-band frequency

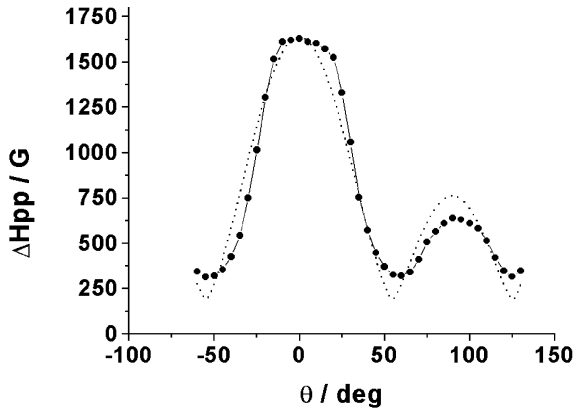

Fig. 4 Angular dependence of the peak-to-peak linewidth ΔH_{pp} of $[Mn(Menic)_2(N_3)_2]_n$ (**1**) at room temperature and at the X-band frequency. Dotted lines show the angular dependence $[3\cos^2\theta - 1]^{4/3}$ for the chain. The solid line is a guide for the eye.

For the single-crystal experiment a well-formed needle in which the chain direction corresponds to the elongation axis of the prism was used. The spectra were recorded by rotating 180° in steps of 5° in an arbitrary plane containing the parallel and perpendicular chain directions. A second rotation around the perpendicular chain direction was also performed. The angular dependence of the peak-to-peak width (ΔH_{pp}) for the first rotation is shown in Fig. 4.

Maximum broadening was found in the parallel direction, ΔH_{pp} = 1628 G, a well-defined minimum in the linewidth was found at the magic angle θ = 54.7°, ΔH_{pp} = 320 G, and a local maximum along the direction perpendicular to the chain, ΔH_{pp} = 640 G. This is the expected behavior for one-dimensional magnets in which spin diffusion determines a large secular enhancement.[42] The angular variation of the linewidth is consistent with the $\Delta H_{pp} = a + b\,(3\cos^2\theta - 1)^{4/3}$ dependence as expected.[41] The best fit values were a = 185 G, b = 577 G. Further confirmation of the one-dimensional behavior comes from the analysis of the lineshape, which is Lorentzian at the magic angle. Some deviation from the Lorentzian shape is observed at θ = 90° and it is diffusive at θ = 0° (Fig. 5).

The second rotation around the chain axis shows only a minor variation in the linewidth in the 180° rotation (100 G approximately). The important information that emerges from the ESR spectra is linked to the fact that the lineshape, following the characteristic one dimensional behavior, provides an upper limit[43] to the interchain exchange interaction,

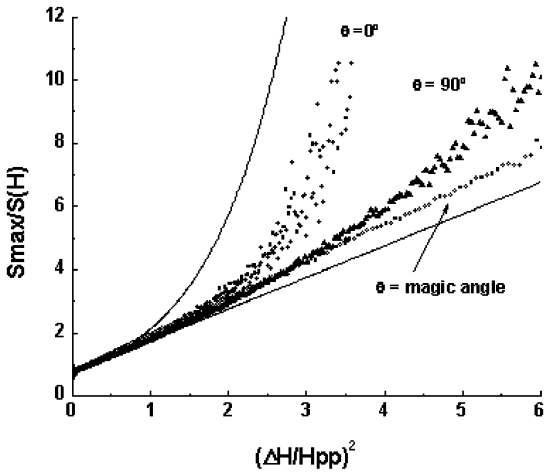

Fig. 5 Lineshape for compound **1**, corresponding to the magic angle and the parallel and perpendicular chain directions. Solid lines show the ideal Gaussian and Lorentzian limits.

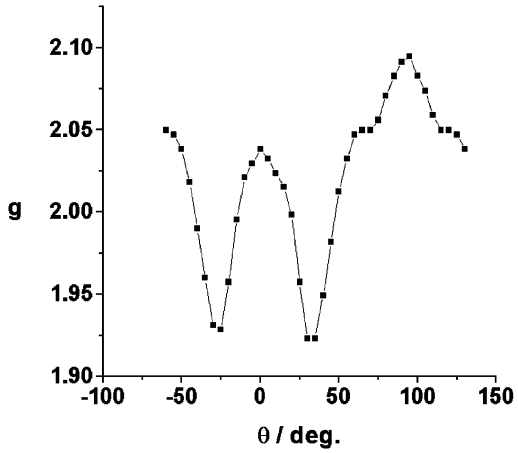

Fig. 6 Angular dependence of the g value for $[Mn(Menic)(N_3)_2]_n$ (**1**) at room temperature and X-band frequency.

J', which would restore the Lorentzian lineshape as $J'/J \leq 10^{-3}$.

The previously studied $[Mn(2\text{-bzpy})_2(N_3)_2]_n$ chain with only EO double azido bridges shows extreme angular variations of the g parameter and from topological similitude and the 2.03 powder value observed for $[Mn(2\text{-bzpy})_2(N_3)_2]_n$, the angular g dependence was also checked in the parallel-perpendicular rotation. The g dependence *vs.* θ is plotted in Fig. 6, which shows a maximum of g = 2.095 at θ = 90°, g = 2.038 for θ = 0° and a minimum value of 1.925 around θ = 25°, in good agreement with the angular dependence of g pointed out by Benner *et al.* for TMMC.[44] These authors suggested that at low symmetry and in the presence of broad lines, the transverse dynamic susceptibility $\chi^{xx}(\omega)$ cannot be efficiently described by the circular polarized susceptibility $\chi^{+\,+}(\omega)$, which is generally used in theoretical treatments. They showed that in some cases the non-diagonal contributions, $\chi^{+\,-}(\omega)$ and $\chi^{-\,+}(\omega)$, must be taken into account. When this is done, dynamic shifts may be observed in the lines. In fact, small shifts were observed in TMMC and $CsMnF_3$.[44]

Monte Carlo calculations

From the viewpoint of magnetism, compound **1** is an alternating one-dimensional system, where the alternation is due to the presence of different coordination modes of the azido bridging ligands. In the chain we found a 1 : 4 ratio for the μ-1,3-azido and μ-1,1-azido ligands connecting the manganese(II) ions.

So, for simplicity, neglecting the small differences in the structural parameters that play an important role in the control of the exchange interaction magnitude [the Mn–N(azido)–Mn angle, in this case], the following interaction topology was chosen to simulate the magnetic behavior of compound **1** (see Scheme 2, topology B). Therefore, the spin Hamiltonian was simplified, giving:

$$H = \sum_{i=0}^{\infty} -(J_1 S_{5i+1}\cdot S_{5i+2} + J_2 S_{5i+2}\cdot S_{5i+3} + J_2 S_{5i+3}\cdot S_{5i+4} + J_2 S_{5i+4}\cdot S_{5i+5} + J_2 S_{5i+5}\cdot S_{5i+6}) \quad (4)$$

where N spins S_i at a lattice site i interact with their nearest neighbors with the exchange coupling constant J_n. To our knowledge, there are no laws for this interaction topology.

In the same way as in the Monte Carlo simulation, to perform a quantitative comparison with the quantum systems, the classical spin has been scaled according to the factor:[16]

$$S_i \Rightarrow \sqrt{S_i(S_i+1)} \quad (5)$$

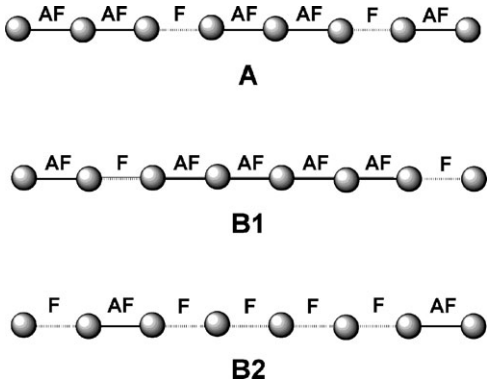

Scheme 2

Fisher[16] has shown that the spin pair correlation function between two interacting neighboring spins, for a finite system in zero field, is given by the Langevin function:

$$\langle S_i S_{i+1} \rangle = \mathrm{Coth}(x) - 1/x \qquad (6)$$

with $x = JS_i(S_i + 1)/T$, where J and T the exchange coupling constant and the temperature, respectively.

So, in this case, the pair correlation function between the spin operators located at sites i and $i + j$ is:

$$\langle S_i S_{i+j} \rangle = u_1 u_2 u_2 u_2 u_2 u_1 u_2 u_2 u_2 u_2 \ldots \qquad (7)$$

where u_1 and u_2 represent to the Langevin functions for the J_1 and J_2 exchange coupling constants, respectively.

On the other hand, the general wave-vector-dependent susceptibility[45] is given by

$$S(q) = \frac{1}{NkT} \sum_{i,j} \langle S_i S_{i+j} \rangle \exp(iqj) \qquad (8)$$

which, in our particular case and in the $q = 0$ limit, is written as follows:

$$S(q) = 1/NkT[5 + \sum_{r=0}^{\infty} (2[u_1^{r+1}u_2^{4r} + 4u_1^r u_2^{4r+1} + 2u_1^{r+1}u_2^{4r+1} + 3u_1^r u_2^{4r+2} + 3u_1^{r+1}u_2^{4r+2} + 2u_1^r u_2^{4r+3} + 4u_1^{r+1}u_2^{4r+3} + u_1^r u_2^{4r+4} + 5u_1^{r+1}u_2^{4r+4}])] \qquad (9)$$

r being an integer number that allows one to consider the different pair correlation functions generated for the topology B.

The integration of this series allows us to deduce the expression for the bulk susceptibility per site (corresponding to the $q = 0$ limit):

$$\chi_M T = \frac{Ng^2 S(S+1)}{15k} \cdot \frac{D}{(1 - u_1 u_2^4)} \qquad (10)$$

where

$$D = 5 + 2u_1 + 8u_2 + 4u_1 u_2 + 6u_2^2 + 6u_1 u_2^2 + 4u_2^3 + 8u_1 u_2^3 + 2u_2^4 + 5u_1 u_2^4$$

It is important to stress that this expression reduces to the classical expressions for a dinuclear species and three isolated ions or a uniform pentanuclear chain when $u_2 = 0$, $u_1 = 0$ or $u_1 = u_2$, respectively.

In a recent paper,[7b] Abu-Youssef *et al.* concluded that some alternating ferro-antiferromagnetic homometallic one-dimensional systems present similar magnetic behavior as the ferrimagnetic chain, defined by Verdaguer *et al.*[11] as a system that contains two different magnetic ions with near-neighboring antiferromagnetic exchange coupling. Thus, with a topology type A (see Scheme 2) with ferromagnetic interactions weaker than the antiferromagnetic interactions, the curve $\chi_M T$ *vs.* T shows a minimum that is a typical signature of a ferrimagnetic 1D system.[7b] For stronger ferromagnetic interactions, this minimum appears after reaching a maximum at higher temperatures.

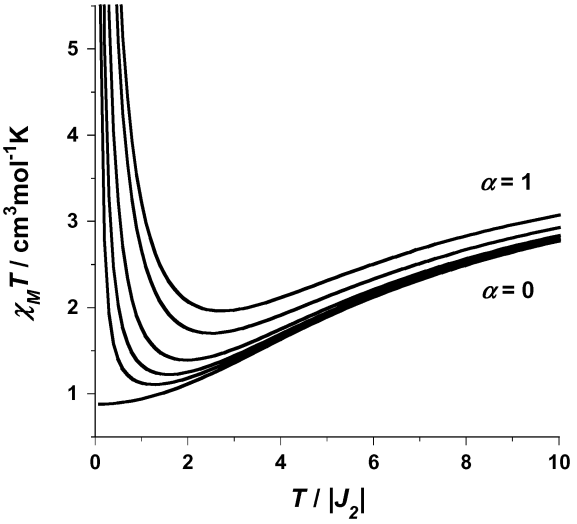

Fig. 7 Thermal variation of the product $\chi_M T$ (χ_M being the magnetic susceptibility per one local spin moment $S_i = 5/2$) of a system with interaction topology type B1 ($J_1 > 0$ and $J_2 < 0$), for different values of the α parameter: 0, 0.05, 0.1, 0.2, 0.5 and 1.0, α being the ratio $J_1/|J_2|$.

Abu-Youssef *et al.*[7b] also proposed several pseudoferromagnetic systems with the azido as bridging ligand, profiting from its capability to coordinate in different ways (μ-1,3-azido and μ-1,1-azido). One of these is an $J_1/J_2/J_2/J_2/J_2$ alternating chain with two possible magnetic interactions (topologies B1 and B2, Scheme 2), which can serve as an interaction model for compound **1**. As found by Abu-Youssef *et al.*[7b] for topology B1, we have also found a minimum in $\chi_M T$ (see Fig. 7).

The magnetic behavior can be understood in the light of the spin configurations present at each temperature (see Fig. 8). (a) A constant value for $\chi_M T$ is expected at high temperature because the influence of the interactions is negligible and full thermal disorder is obtained, corresponding to the free behavior of the spins. (b) For weak ferromagnetic interactions, since the stronger antiferromagnetic coupling promotes the antiparallel spin configuration, the $\chi_M T$ product decreases when cooling (see Fig. 8). (c) A minimum is reached due to the parallel alignment promoted by the weaker ferromagnetic interactions, which are effective at low temperature (see Fig. 8). The stronger antiferromagnetic interaction leads to a paramagnetic ground state $S = 5/2$ for a pentanuclear unity. The weaker ferromagnetic interaction connects this units in a ferromagnetic way, leading to a divergence of $\chi_M T$.

On the other hand, the magnetic behavior in the topology type B2 is not so simple as in type A or B1. We have found a maximum at lower temperatures (Fig. 9). This apparently

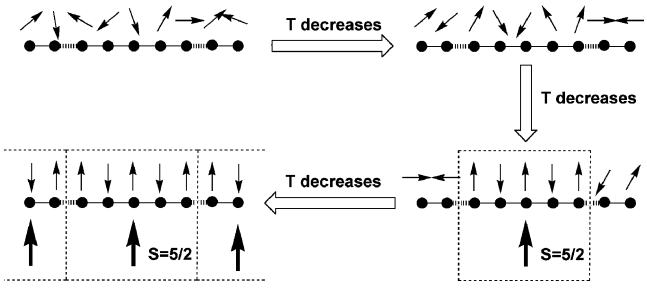

Fig. 8 Thermal variation of the spin configuration for a topology type B1. The antiferro- and ferromagnetic interactions are represented by solid and dashed lines, respectively.

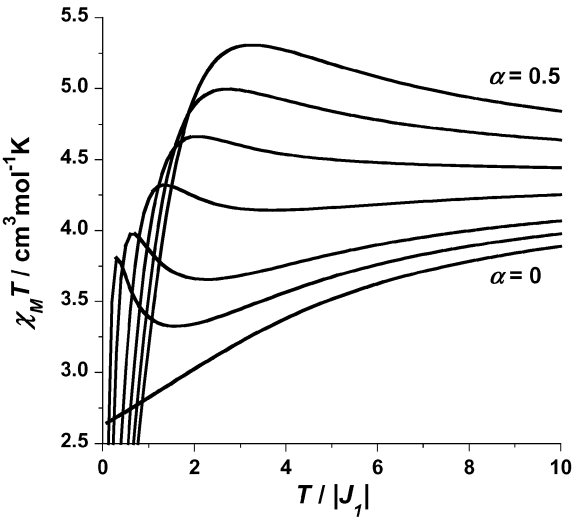

Fig. 9 Thermal variation of the product $\chi_M T$ (χ_M being the magnetic susceptibility per one local spin moment $S_i = 5/2$) of a system with interaction topology type B2 ($J_1 < 0$ and $J_2 > 0$), for different values of the α parameter: 0, 0.05, 0.1, 0.2, 0.3, 0.4 and 0.5, α being the ratio $J_2/|J_1|$.

anomalous magnetic behavior is explained in the following ways. (a) In the same way as in topology B1, the stronger antiferromagnetic coupling promotes the antiparallel spin configuration, so the $\chi_M T$ product decreases when cooling (see Fig. 10). (b) At lower temperatures, in spite of the weak character of the ferromagnetic interactions, the ferromagnetic alignment of the resulting spins becomes efficient (see Fig. 10) since these are present in a greater proportion (4 : 1). (c) Finally, the stronger interaction dominates the magnetic behavior, such that $\chi_M T$ increases to reach a maximum and decreases subsequently to a zero value at 0 K. In this interval of temperature the ferromagnetic correlation tries to populate the spin ground state for a ferromagnetic pentanuclear $S = 25/2$. However, at the same time, the antiferromagnetic interaction tries to annihilate this effect into a pentanuclear unit opposing the neighboring units. So, a ground state S_T and a $\chi_M T = 0$ value are expected (see Fig. 10). Since the ratio between the ferro- and antiferromagnetic interactions is 4 : 1, a minimum of $\chi_M T$ is not observed for α values greater than 0.25.

This theoretical behavior is observed for **1**. The $\chi_M T$ curve as a function of temperature [see Fig. 2 (plots 3, 4)] exhibits a minimum and a maximum at 55 and 10 K, respectively. The best agreement between the magnetic data and eqn. (10) in the temperature range of 300–30 K is obtained with the following parameters: $g = 2.042 \pm 0.003$, $J_1 = -17.7 \pm 0.4$ cm^{-1} and $J_2 = 1.669 \pm 0.020$ cm^{-1}. The agreement factor F, defined as:

$$F = \sum \left[(\chi_M T)_{obsd} - (\chi_M T)_{calcd}\right]^2 \Big/ \sum \left[(\chi_M T)_{obsd}\right]^2$$

is equal to 1.1×10^{-5}.

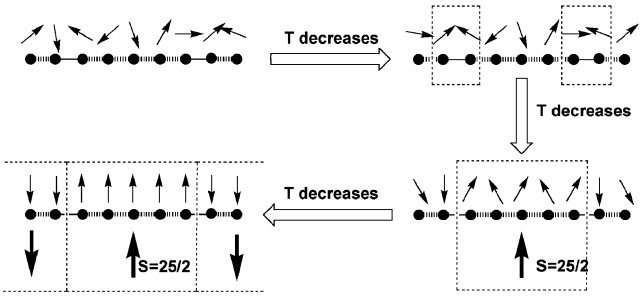

Fig. 10 Thermal variation of the spin configuration for a topology type B2. The antiferro- and ferromagnetic interactions are represented by solid and dashed lines, respectively.

A Monte Carlo simulation of $\chi_M T$ as a function of T has been done using the parameters obtained in the previous fit. A perfect agreement is found between the two simulations. Fig. 2 (plots 3 and 4) shows that eqn. (10) is not able to describe properly the maximum in $\chi_M T$. A fit including the intermolecular interactions (θ parameter) has been done in the temperature range of 300–4 K and a quite fair description of the curve is obtained ($g = 2.077 \pm 0.010$, $J_1 = -19.1 \pm 1.3$ cm^{-1} and $J_2 = 1.144 \pm 0.024$ cm^{-1}, $\theta = -0.61 \pm 0.04$ cm^{-1} and $F = 3.0 \times 10^{-4}$). However, the crystal structure shows that the manganese(II) chains are isolated chains (shortest interchain Mn···Mn distances: 10.857 and 11.723 Å) in opposition to the very large value obtained for θ. In the same way, the single-crystal ESR study shows that the interchain exchange coupling is one thousand times smaller than that of the intrachain coupling. Moreover, the g factor obtained from the fit is too high for the known manganese(II) complexes. On the other hand, we can consider different g factors for each one of the independent manganese(II) ions. In this case, we cannot compensate the spin moments and the one-dimensional system will not show a diamagnetic behavior at 0 K. Moreover, slight shifts in the position of the minimum of $\chi_M T$ could be observed. Nevertheless, the manganese(II) ions present g factors very close to 2.0 and possible slight deviations from this value cannot be observed in the $\chi_M T$ *vs.* T curve.

As we have seen in the structural description, a more detailed structural analysis shows that the Mn–N [(μ-1,1-azido)–Mn angles (α angles)] are not equivalent throughout the chain. In fact, a $J_1/J_2/J_2/J_3/J_3$ topology (C in Scheme 3; the dashed box represents the translational unit) is more correct to describe the magnetic properties of **1**. However, the experimental α angles in **1** are not very different between them and similar values for the exchange coupling constants should be consistent with structural data.

In the same way as for topology B1, we have obtained for topology C a law able to relate the $\chi_M T$ product to temperature. To do so, we have used the following Hamiltonian and general wave-vector-dependent susceptibility:

$$H = \sum_{i=0}^{\infty} -(J_1 S_{5i+1} \cdot S_{5i+2} + J_2 S_{5i+2} J_2 S_{5i+3} \cdot S_{5i+4} + J_3 S_{5i+4} \cdot S_{5i+5} + J_3 S_{5i+5} \cdot S_{5i+6}) \quad (11)$$

$$\begin{aligned} S(q) = 1/NkT[5 + \sum_{r=0}^{\infty} \big(2\big[&u_1^{r+1}u_2^{2r}u_3^{2r} + 2u_1^{r}u_2^{2r+1}u_3^{2r} \\ &+ 2u_1^{r}u_2^{2r}u_3^{2r+1} + u_1^{r}u_2^{2r}u_3^{2r+2} + 2u_1^{r+1}u_2^{2r+1}u_3^{2r} \\ &+ 2u_1^{r}u_2^{2r+1}u_3^{2r+1} + 2u_1^{r}u_2^{2r+1}u_3^{2r+2} + u_1^{r+1}u_2^{2r+2}u_3^{2r} \\ &+ 2u_1^{r+1}u_2^{2r+1}u_3^{2r+1} + u_1^{r}u_2^{2r+2}u_3^{2r+2} + 2u_1^{r+1}u_2^{2r+1}u_3^{2r+2} \\ &+ 2u_1^{r+1}u_2^{2r+2}u_3^{2r+1} + 5u_1^{r+1}u_2^{2r+2}u_3^{2r+2}\big]\big)\big] \end{aligned} \quad (12)$$

in which u_1, u_2 and u_3 are the Langevin functions for the J_1, J_2 and J_3 exchange constants, to give the following expression for the $\chi_M T$ product for topology C:

$$\chi_M T = \frac{Ng^2 S(S+1)}{15k} \cdot \frac{D}{(1 - u_1 u_2^2 u_3^2)} \quad (13)$$

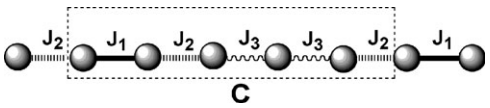

C

Scheme 3

where

$$D = 5 + 2u_1 + 4u_2 + 4u_3 + 4u_1u_2 + 4u_2u_3 + 2u_3^2 + 2u_1u_2^2 + 4u_2u_3^2 + 4u_1u_2u_3 + 4u_1u_2u_3^2 + 4u_1u_2^2u_3 + 2u_2^2u_3^2 + 5u_1u_2^2u_3^2$$

In order to check the validity of eqn. (13) we have verified that this reduces to eqn. (10) when $u_2 = u_3$.

The least-square analysis (300–8 K) of the $\chi_M T$ data for **1** using the eqn. (13) leads to $g = 2.036 \pm 0.004$, $J_1 = -15.6 \pm 0.5$ cm^{-1}, $J_2 = 1.059 \pm 0.014$ cm^{-1}, $J_3 = 1.556 \pm 0.016$ cm^{-1} and $F = 3.0 \times 10^{-5}$ (see Fig. 2, plots 1, 2). The Monte Carlo simulation using these parameters is in agreement with the simulation using the theoretical law in eqn. (13). Now, the full curve of $\chi_M T$ *vs.* T is correctly described by the theoretical law. However, this might be a mathematical artifice because we have added a new parameter, giving more flexibility to the analytical expression. In order to check the validity of the model we have done an analysis of the values of the exchange coupling constants. The interactions through the μ-1,1 and μ-1,3-azido bridges are similar to those found in simpler systems. There are few examples in the literature of manganese(II) complexes with a double μ-1,3-azido group as bridging ligand,[5a,6,46–50] and for all of them, exchange coupling constants lie in the −7 to −15 cm^{-1} range. The value of J_1 obtained by us is in agreement with these values found in the literature.

For the double μ-1,1-azido bridge, we have obtained similar (but not identical) J values (1.06 and 1.56 cm^{-1}). This is in agreement with our idea that the small structural differences (α angle, 100.6° and 101.1°) imply small changes in the J values. A few compounds with the [Mn–(μ-1,1-N_3)$_2$–Mn] structural motif are known. They present several topologies: three-dimensional stacked honeycomb,[46] bi-dimensional honeycomb,[19,51,52] double chain,[46] one-dimensional[7b,19,48,53] and dinuclear.[50] The J and α values are found in the ranges 0.76–4.9 cm^{-1} and 99.2–104.6°, respectively. In Fig. 11 is shown the magnetic-structural correlation between the J values an the α angle. It can be observed that the J value is smaller for small α values, in agreement with the DFT calculations performed by Ruiz *et al.*,[36] who proposed a crossover from ferro- to antiferromagnetic interactions at 98.5°. The J values obtained by us for **1** using eqn. (13) are in good agreement with this correlation. So, the bigger J value corresponds to the bigger α angle (see structural parameters and topology scheme), giving validity to the model of interaction type C and showing that the parameter has a physical meaning and is not a result of a mathematical artifice. It is important to emphasize that small exchanges in the J_2 and J_3 values are capable of promoting large changes in the $\chi_M T$ *vs.* T plots.

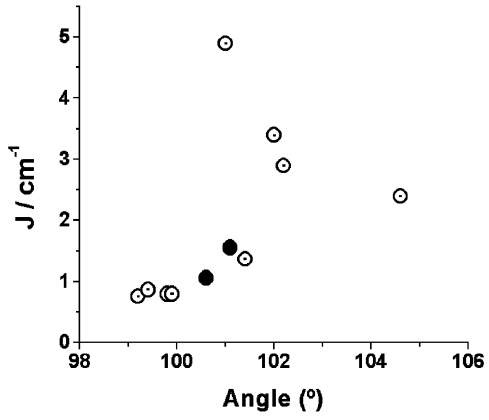

Fig. 11 Magneto-structural correlation between the J exchange coupling constant and the α angle in the [Mn–(μ-1,1-N_3)$_2$–Mn] motif. The compounds shown are: **1** (black circles), $Cs_n[\{Mn(N_3)_3\}_n]$,[46] $[\{N(C_2H_5)_4\}_n][\{Mn_2(N_3)_5(H_2O)\}_n]$,[46] *trans*-$[Mn(3\text{-Mepy})_2(N_3)_2]_n$,[7b] *trans*-$[Mn(3,4\text{-Dmepy})(N_3)_2]_n$,[7b] $[\{Mn(2\text{-bzpy})(N_3)_2\}_n]$,[5a] $[Mn(bipy)(N_3)_2]_n$,[19,48,53] $[Mn(bpm)(N_3)_2]_n$,[19,51] $[Mn(4\text{-Etpy})_2(N_3)_2]_n$[52] and $[\{Mn(terpy)(\mu\text{-}1,1\text{-}N_3)\}(N_3)_2]$.[50]

Conclusions

The synthesis, structure, ESR and magnetic studies of a one-dimensional manganese(II) compound are presented here. This compound shows a peculiar interaction topology due to the different coordination modes of the azide ligand. The theoretical studies of the magnetic properties show that these interaction topologies, where ferro- and antiferromagnetic interactions coexist, allow the appearance of magnetic behavior in a homopolynuclear system similar to the ferrimagnetic behavior observed in heteropolynuclear systems. Exact laws have been obtained to elucidate and analyze the magnetic behavior. We have checked that Monte Carlo methods are also efficient to describe the magnetic behavior; they can be used whenever exact laws cannot be deduced

Acknowledgements

J. C. and Y. J. thank the EU for support under the TMR Program "Molecules as Nanomagnets" (HPRN-CT-1999-00012). A.E. and R.V. thank the Ministerio de Ciencia y Tecnología (Spain), project BQU2003/0538, for financial support of this research. F. M. thanks OENB (project 7967) for financial support.

References

1 J. Ribas, A. Escuer, M. Monfort, R. Vicente, R. Cortés, L. Lezama and T. Rojo, *Coord. Chem. Rev.*, 1999, **193–195**, 1027.
2 (*a*) Z. H. Zhang, X. H. Bu, Z. H. Ma, W. M. Bu, Y. Tang and Q. H. Zhao, *Polyhedron*, 2000, **19**, 1559; (*b*) Z. E. Serna, L. Lezama, M. K. Urtiaga, M. I. Arriortua, M. G. Barandika, R. Cortés and T. Rojo, *Angew. Chem., Int. Ed.*, 2000, **39**, 344; (*c*) G. S. Papaefstathiou, S. P. Perlepes, A. Escuer, R. Vicente, M. Font-Bardia and X. Solans, *Angew. Chem. Int. Ed.*, 2001, **40**, 884; (*d*) G. S. Papaefstathiou, A. Escuer, C. P. Raptopoulou, A. Terzis, S. P. Perlepes and R. Vicente, *Eur. J. Inorg. Chem.*, 2001, 1567.
3 (*a*) S. Han, J. L. Manson, J. Kim and J. S. Miller, *Inorg. Chem.*, 2000, **39**, 4182; (*b*) M. A. S. Goher, M. A. M. Abu-Youssef, F. A. Mautner, R. Vicente and A. Escuer, *Eur. J. Inorg. Chem.*, 2000, 1819; (*c*) A. K. Sra, J. P. Sutter, P. Guionneau, D. Chasseau, J. V. Yakhmi and O. Kahn, *Inorg. Chim. Acta*, 2000, **300–302**, 778; (*d*) M. L. Hernández, M. G. Barandika, M. K. Urtiaga, R. Cortés, L. Lezama and M. I. Arriortua, *J. Chem. Soc., Dalton Trans.*, 2000, 79; (*e*) M. Villanueva, J. L. Mesa, M. K. Urtiaga, R. Cortés, L. Lezama, M. I. Arriortua and T. Rojo, *Eur. J. Inorg. Chem.*, 2000, 1581.
4 A. Escuer, R. Vicente, F. A. Mautner, M. A. S. Goher and M. A. M. Abu-Youssef, *Chem. Commun.*, 2002, 64.
5 (*a*) M. A. M. Abu-Youssef, A. Escuer, D. Gatteschi, M. A. S. Goher, F. A. Mautner and R. Vicente, *Inorg. Chem.*, 1999, **38**, 5716; (*b*) J. L. Manson, A. M. Arif and J. S. Miller, *Chem. Commun.*, 1999, 1479.
6 A. Escuer, R. Vicente, M. A. S. Goher and F. A. Mautner, *Inorg. Chem.*, 1998, **37**, 782.
7 (*a*) M. A. M. Abu-Youssef, A. Escuer, M. A. S. Goher, F. A. Mautner, G. Reiβ and R. Vicente, *Angew. Chem. Int. Ed.*, 2000, **39**, 1624; (*b*) M. A. M. Abu-Youssef, M. Drillon, A. Escuer, M. A. S. Goher, F. A. Mautner and R. Vicente, *Inorg. Chem.*, 2000, **39**, 5022.
8 (*a*) L. F. Tang, L. Zhang, L. C. Li, P. Cheng, Z. H. Wang and J. T. Wang, *Inorg. Chem.*, 1999, **38**, 6326; (*b*) H. Y. Shen, W. M. Bu, E. Q. Gao, D. Z. Liao, Z. H. Jiang, S. P. Yan and G. L. Wang, *Inorg. Chem.*, 2000, **39**, 396; (*c*) M. A. M. Abu-Youssef, A. Escuer, M. A. S. Goher, F. A. Mautner and R. Vicente, *J. Chem. Soc., Dalton Trans.*, 2000, 413.
9 *Extended Linear Chain Compounds*, ed. J. S. Miller, Plenum, New York, 1983, vol. **3**.
10 A. Glezes and M. Verdaguer, *J. Am. Chem. Soc.*, 1981, **103**, 7373.
11 M. Vedaguer, M. Julve, A. Michalowicz and O. Kahn, *Inorg. Chem.*, 1983, **22**, 2624.
12 M. Drillon, E. Coronado, R. Georges, J. C. Gianguzzo and J. Curely, *Phys. Rev. B.*, 1989, **40**, 10992.

13 K. Maisinger, U. Shollwöck, S. Brehmer, H. J. Mikeska and S. Yamamoto, *Phys. Rev. B*, 1998, **58**, 5908.
14 S. Yamamoto and T. Fukui, *Phys. Rev. B*, 1998, **57**, 14008.
15 A. S. Ovchinnikov, I. G. Bostrem, V. E. Sinitsyn, A. S. Boyardekkov, N. V. Bararnov and K. Inoue, *J. Phys. Condens. Matter.*, 2002, **14**, 8067.
16 M. E. Fisher, *Am. J. Phys.*, 1964, **32**, 343.
17 R. Cortés, M. K. Urtiaga, L. Lezama, J. L. Pizarro, M. I. Arriortua and T. Rojo, *Inorg. Chem.*, 1997, **36**, 5016.
18 (*a*) J. Curély, *Physica B*, 1998, 277; (*b*) J. Curély, F. Lloret and M. Julve, *Phys. Rev. B*, 1998, **58**, 11465.
19 J. Cano-Boquera and Y. Journaux, *Mol. Cryst. Liq. Cryst.*, 1999, **335**, 685.
20 M. Suzuki, *Quantum Monte Carlo Methods*, Springer–Verlag, Heidelberg, Germany, 1986.
21 M. Suzuki, *Phys. Rev. B*, 1985, **31**, 2957.
22 M. Suzuki, *Prog. Theor. Phys.*, 1976, **56**, 1454.
23 J. E. Hirsch, R. L. Sugar, D. J. Scalapino and R. Blankenbecler, *Phys. Rev. B*, 1982, **26**, 5033.
24 S. Yamamoto, *Phys. Rev. B*, 1996, **53**, 3364.
25 S. Yamamoto, *Phys. Rev. B*, 1995, **52**, 10170.
26 M. S. Makivic and H. Q. Ding, *Phys. Rev. B*, 1991, **43**, 3562.
27 K. Binder and D. W. Hermann, *Monte Carlo Simulations in Statistical Physics. An Introduction*, Springer, 3rd edn., Heidelberg, 1997.
28 K. Binder, *The Monte Carlo Method in Condensed Matter Physics*, Springer–Verlag, Heidelberg, Germany, 1996, vol. **71**.
29 S. R. White and R. M. Noack, *Phys. Rev. Lett.*, 1992, **68**, 3487.
30 S. R. White and D. H. Huse, *Phys. Rev. B*, 1993, **48**, 3844.
31 S. R. White, *Phys. Rev. B*, 1993, **48**, 10345.
32 S. R. White, *Phys. Rev. Lett.*, 1992, **69**, 2863.
33 U. Schollwöck, O. Golinelli and T. Jolicoeur, *Phys. Rev. B*, 1996, **54**, 4038.
34 S. K. Pati, S. Ramesha and D. Sen, *Phys. Rev. B*, 1997, **55**, 8894.
35 N. Metropolis, A. W. Rosebluth, M. N. Rosenbluth, A. H. Teller and E. Teller, *J. Chem. Phys.*, 1953, **21**, 1087.
36 E. Ruiz, J. Cano, S. Alvarez and P. Alemany, *J. Am. Chem. Soc.*, 1998, **120**, 11122.
37 *STOE-IPDS-Software*, STOE & Cie GmbH, Darmstadt, Germany, 1998.
38 *SHELXTL 5.03 (PC Version), Program Library for Structure Solution and Molecular Graphics*, Siemens Analytical Instruments Division, Madison, WI, USA, 1995.
39 G. M. Sheldrick, *SHELXL-97, Program for refinement of crystal structures*, University of Göttingen, Germany, 1997.
40 H. Gould and J. Tobochnik, *An Introduction to Computer Simulation Methods. Applications to Physical Systems*, Addison–Wesley, 1996.
41 A. Bencini and D. Gatteschi, *EPR of Exchange Coupled Systems*, Springer–Verlag, Berlin and Heidelberg, Germany, 1990, ch. 10 and references therein.
42 (*a*) H. Kalt, E. Siegel, N. Pauli, H. Mosebach, J. Wiese and A. Edgar, *J. Phys. C*, 1983, **16**, 6427; (*b*) P. M. Richards, R. K. Quinn and B. Morosin, *J. Chem. Phys.*, 1973, **59**, 4474.
43 M. J. Hennessy, C. D. McElwee and P. M. Richards, *Phys. Rev. B*, 1973, **7**, 930.
44 H. Benner, M. Brodehl, H. Seitz and J. Wiese, *J. Phys. C.*, 1983, **16**, 6011.
45 M. F. Thorpe, *J. Phys.*, 1975, **36**, 1177.
46 M. A. S. Goher, J. Cano, Y. Journaux, M. A. M. Abu-Youssef, F. A. Mautner, A. Escuer and R. Vicente, *Chem.-Eur. J.*, 2000, 778.
47 K. R. Reddy, M. V. Rajasekharan and J. P. Tuchages, *Inorg. Chem.*, 1998, **37**, 5978.
48 G. Viau, M. G. Lombardi, G. De Munno, M. Julve, F. Lloret, J. Faus, A. Caneschi and J. M. Clemente-Juan, *Chem. Commun.*, 1997, 1195.
49 A. Escuer, R. Vicente, M. A. S. Goher and F. A. Mautner, *Inorg. Chem.*, 1996, **37**, 6386.
50 R. Cortés, J. L. Pizarro, L. Lezama, M. I. Arriortua and T. Rojo, *Angew. Chem., Int. Ed. Engl.*, 1994, **33**, 2697.
51 G. De Munno, M. Julve, G. Viau, F. Lloret, J. Faus and D. Viterbo, *Angew. Chem., Int. Ed. Engl.*, 1996, **35**, 1807.
52 A. Escuer, J. Cano, M. A. S. Goher, Y. Journaux, F. Lloret, F. A. Mautner and R. Vicente, *Inorg. Chem.*, 2000, **39**, 4688.
53 R. Cortés, M. Drillon, X. Solans, L. Lezama and T. Rojo, *Inorg. Chem.*, 1997, **36**, 677.